

SIMULATION OF E-CLOUD USING ORBIT: BENCHMARKS AND FIRST APPLICATION*

Y. Sato^{*,*}, A. Shishlo, S. Danilov, J. Holmes, S. Henderson,
SNS^{*,*} project, ORNL, Oak Ridge, TN 37831, USA

Abstract

We have developed an electron cloud module and implemented it in the ORBIT Code for beam dynamics in high intensity rings. In addition to studying the dynamics of the electron cloud, our intent in developing this model is to examine the effect of the electron cloud on the protons. In this presentation, we examine benchmarking and initial applications of the ORBIT electron cloud module to SNS. Specifically, we test the secondary emission surface model and compare instability results with an analytically solvable two-stream model. By taking these benchmarks into account, we also discuss the estimation of computational requirements for a PSR bunched beam case.

ELECTRON CLOUD MODULE

A new electron cloud module, designed to simulate the self consistent dynamics of the proton beam and the electrons, has been implemented in ORBIT [1]. The secondary electron emission process is calculated using an implementation of the model of Furman and Pivi [2]. We benchmark this model by comparing the secondary energy spectrum and the electron cloud development for a cold proton beam to Pivi and Furman's results [3]. The instability caused by an electron cloud effect (ECE) may reduce the performance of high intensity proton storage rings, such as the Proton Storage Ring (PSR) at the Los Alamos National Laboratory [4] and the Spallation Neutron Source accumulation ring. We simulate the electron-proton instability for an analytically solvable model, the two-stream model [5], using the SNS parameters. We estimate the computational requirements to simulate the PSR bunched beam case by extrapolating from the benchmark of the two-stream model.

BENCHMARK: SECONDARY EMISSION SURFACE MODEL IN ORBIT

We implemented the secondary emission surface model of Furman and Pivi into ORBIT using their parameterization but a modified Monte Carlo scheme to save calculation time. The basic feature of the model is to remove the electron-macroparticle hitting the surface from the electron bunch and to add a new electron-macroparticle with its macrosize multiplied by the

secondary emission yield (SEY), δ , compared to the macrosize of the removed electron-macroparticle, and with its energy determined by sampling from the model spectrum. We use a flexible Monte Carlo scheme to control the number of macroparticles and their macrosize without changing the physics of the model.

Furman and Pivi's model

As in the Furman and Pivi model, ORBIT divides the total SEY, $\delta = I/I_0$, into three components: elastic backscattered electrons $\delta_{el} = I_{el}/I_0$, rediffused electrons $\delta_{rd} = I_{rd}/I_0$ and true secondary electrons $\delta_{ts} = I_{ts}/I_0$, so that

$$\delta(E_0, \theta_0) = \delta_{el} + \delta_{rd} + \delta_{ts} = I/I_0. \quad (1)$$

Here, I_0 is the incident electron beam current and I is the secondary current, which consists of I_{el} , the elastic back scattered current, I_{rd} , the rediffused current, and I_{ts} , the true secondary current. Each component has its own particular spectrum [2]. To determine the energy of emitted electron-macroparticle, we choose the type of emission first and then obtain the energy from its spectrum through random sampling. The choice of emission type depends on the following probabilities:

$$P_{\text{elastic backscattered}} = \delta_{el}/\delta \quad (2a)$$

for elastic backscattered emission,

$$P_{\text{rediffused}} = \delta_{rd}/\delta \quad (2b)$$

for rediffused emission, and

$$P_{n, \text{true secondary}} = \left(\frac{\delta_{ts}}{\delta} \right) \cdot \frac{P_{n,ts}}{\sum_{i=1}^{M_{\text{emiss}}} P_{i,ts}} \quad (2c)$$

for n -th true secondary emission, where n is the number of secondary electrons per event, $1 \leq n \leq M_{\text{emiss}}$, and

$$P_{n,ts} = \binom{M_{\text{emiss}}}{n} \left(\frac{\delta_{ts}}{M_{\text{emiss}}} \right)^n \left(1 - \frac{\delta_{ts}}{M_{\text{emiss}}} \right)^{M_{\text{emiss}} - n}. \quad (2d)$$

They satisfy

* Research sponsored by UT-Batelle, LLC, under contract no. DE-AC05-00OR22725 and DE-FG02-92ER40747 for the U.S. Department of Energy, and NSF under contract no. PHY-0244793.

*^s satoy@ornl.gov, Indiana University, Bloomington

*^{rs} SNS is a partnership of six national laboratories: Brookhaven, Argonne, Jefferson, Lawrence Berkeley, Los Alamos and Oak Ridge.

$$P_{\text{elastic backscattered}} + P_{\text{rediffused}} + \sum_{i=1}^{M_{\text{emiss}}} P_{n, \text{ true secondary}} = 1. \quad (2e)$$

When calculating the energy of true secondary electrons, we simplify the original Furman and Pivi model by assuming the emitted energy is much smaller than the incidental energy.

Secondary energy spectrum

As our benchmark of the surface emission model, we calculate the secondary electron energy spectra from normal incident electrons on copper and stainless steel surfaces and compare the ORBIT results with those of Furman and Pivi [2] (see Figs. 1, 2, 3, 4).

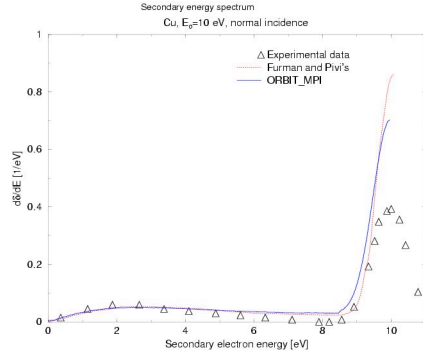


Fig. 1. The emitted energy spectrum for copper at 10 eV incident energy and normal incidence

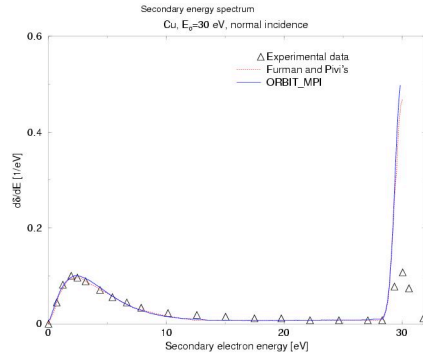


Fig. 2. The emitted energy spectrum for copper at 30 eV incident energy and normal incidence

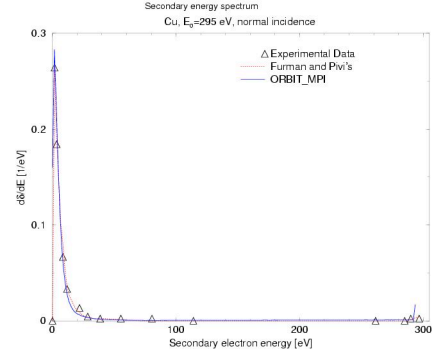


Fig. 3. The emitted energy spectrum for copper at 295 eV incident energy and normal incidence

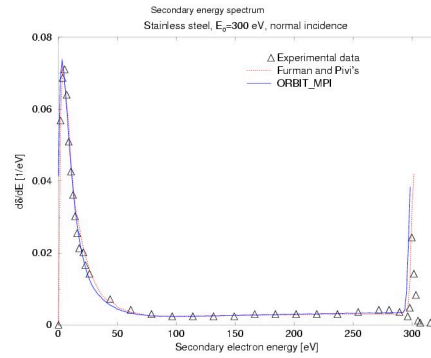


Fig. 4. The emitted energy spectrum for stainless steel at 300 eV incident energy and normal incidence

The ORBIT spectra match Furman and Pivi values quite closely. The Gaussian distribution in the experimental data around the incident energy is a manifestation of the energy resolution of the detector.

Electron Cloud Development in a Cold Proton Bunch

In this section we calculate the electron cloud development without applying kicks to the proton bunch and compare the results with Pivi and Furman [3] results for the same calculation (Fig. 5).

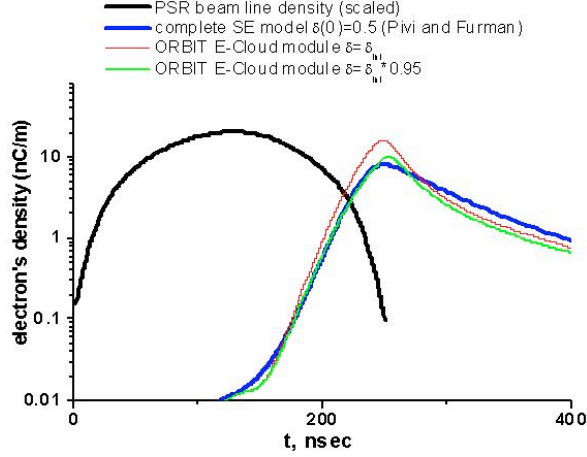


Fig. 5. Electron cloud development in a cold PSR beam pulse with $N_p = 3.12 \times 10^{13}$ and with SEY $\delta_{\max} = 2.0$ and $\delta_{\max} = 1.9$. The peak height of the electron cloud is sensitive to the size of SEY. The Pivi and Furman results were calculated with $\delta_{\max} = 2.0$.

We use the same parameterization as Pivi and Furman but adopt a different Monte Carlo scheme. With the same SEY, the ORBIT electron cloud development attains twice the peak height as the Pivi and Furman calculation. This peak is, however, very sensitive to the value of SEY, and reducing our SEY slightly to 95% of the initial value yields results in close agreement with those of Pivi and Furman.

BENCHMARK OF INSTABILITY FOR TWO STREAM MODEL

We simulate the electron-proton instability for an analytically solvable model, the two-stream model [5], using SNS parameters in our benchmarks.

Analytically Solvable Electron Cloud Model

We assume longitudinally uniform proton and electron distributions. Both streams have uniform elliptical cross section with areas $\pi a_p b_p$ and $\pi a_e b_e$, respectively. We assume harmonic oscillations in both centroid motions in the vertical direction:

$$y_{p,c} = A_p \exp[i(n\theta - \omega t)], \quad (3a)$$

$$y_{e,c} = A_e \exp[i(n\theta - \omega t)], \quad (3b)$$

where n is the longitudinal harmonic number, θ is the angle around the ring and ω is e-p frequency. From the equations of motion, we obtain the complex amplitude ratio

$$A_e/A_p = \frac{\omega_e^2}{\omega_e^2 - \omega^2} \quad (4)$$

and the following dispersion relation under no frequency spread:

$$(\omega_e^2 - \omega^2) \left[\omega_\beta^2 + \omega_p^2 - (n\omega_0 - \omega)^2 \right] = \omega_e^2 \omega_p^2, \quad (5)$$

where ω_β is the betatron frequency, ω_0 is the revolution frequency of protons,

$$\omega_{p,V}^2 = \frac{4\lambda_e r_p c^2}{\gamma b_e (a_e + b_e)}, \quad \omega_{e,V}^2 = \frac{4\lambda_p r_e c^2}{b_p (a_p + b_p)}, \quad (6a, 6b)$$

r_p and r_e are the classical proton and electron radii, and λ_p and λ_e are the line densities of the proton bunch and the electron cloud. This relation was derived assuming linear forces inside the streams. For sufficiently high electron and proton densities, the dispersion relation has complex solutions for values of n , each of which is near $\omega \sim \omega_e \sim (n\omega_0 - \omega_\beta)$, slow wave, and satisfies the threshold condition:

$$\omega_p \gtrsim \omega_0 \sqrt{\frac{Q_\beta}{Q_e}} |n - Q_e - Q_\beta|, \quad (7)$$

where Q_β is the betatron tune and $Q_e = \omega_e/\omega_0$. We find instabilities around the harmonic $n \approx Q_e + Q_\beta$.

Two Stream Model in ORBIT

To study the two-stream model in ORBIT, we use the following parameters, inspired by SNS: $a_e = b_e = a_p = b_p = 30$ mm, betatron tune $Q_x = Q_y = 6.2$, 1 GeV proton beam,

revolution frequency $\omega_0 = 2\pi/T = 6.646 [\mu\text{s}^{-1}]$,

$$\lambda_p = \frac{1.5 \times 10^{14}}{0.65 \times 248 \text{ m}} \cdot (2.5)_{\text{Bunch factor}} = 2.326 \times 10^{12} [\text{m}^{-1}],$$

$$Q_e = \omega_e/\omega_0 = 172.171, \quad Q_p = \omega_p/\omega_0 = 2.79616\sqrt{\eta}, \quad \text{and}$$

neutralization factor $\eta = \lambda_e/\lambda_p$. With these parameters, the greatest instability occurs at longitudinal harmonic number $n = 178 \approx Q_e + Q_y$. For sufficient electron cloud, exceeding the threshold, the dispersion relation for $n = 178$ has a growth mode as one of the four roots of ω :

$$\omega_2/\omega_0 = 171.961 - 0.716i, \quad |A_e/A_p|_{\omega_2} = 116.1$$

for $\eta = 0.01$. The complex amplitude ratio is the function of the neutralization factor shown in Fig. 6.

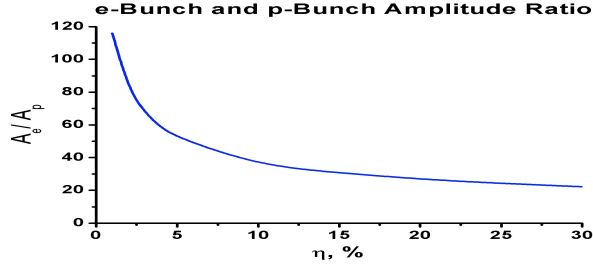


Fig. 6. The absolute amplitude ratio of the two streams

We expect the oscillations of both centroids to grow when we initialize the electron cloud and proton beam as slow waves with $n = 178$ and the proper phase relationship. To reduce the calculation time, we adopt the periodic structure of $L = 248 \text{ mm}/178 = 1.393 \text{ mm}$ and the number of protons $N_p = \lambda_p L = 3.241 \times 10^{12}$. For the electron cloud, we assume 20 computational nodes. The initial proton bunch is a KV distribution, which has 32 point symmetric structure in phase space numerically (16 points from $\pm x, \pm y, \pm p_x, \pm p_y \times 2$ for $(x, p_x) \leftrightarrow (y, p_y)$, and no energy spread. We take radius $R_p = 30 \text{ mm}$, 0.01 mm slow wave centroid modulation in the vertical direction and more than 400,000 macroparticles to satisfy at least 10 macroparticles/grid-cell. The initial electron cloud is a KV distribution with radius $R_e = 26 \text{ mm}$ ($< R_p$), $(A_e/A_p)_{\eta, \text{growth mode}} \times 0.01 \text{ mm}$ slow wave centroid modulation in the vertical direction, 400,000 macroelectrons and $\lambda_e = \eta (R_e/R_p) \lambda_p$. The reason we take $R_e < R_p$ is to maintain force linearity on the electrons, which undergo the greater oscillations, as we seek the coherent centroid growth in both streams. The following benchmark of the proton bunch motion passing through a cold uniform electron cloud (Fig. 7) shows the force nonlinearity near the edge of the streams.

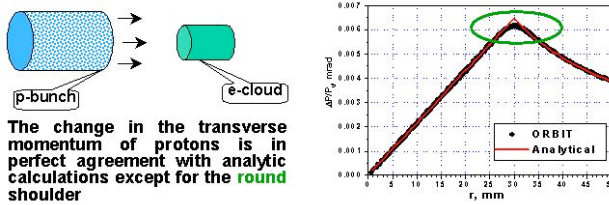


Fig. 7. Benchmark of the electrostatic force inside the uniform stream.

The radius difference does not change Q_e and Q_p because we redefined the neutralization factor as $\eta = (R_p/R_e) (\lambda_e/\lambda_p)$.

Results: Centroid motion

The centroid oscillations of the electron cloud and the proton bunch undergo coherent growth for the first several turns (Fig. 8).

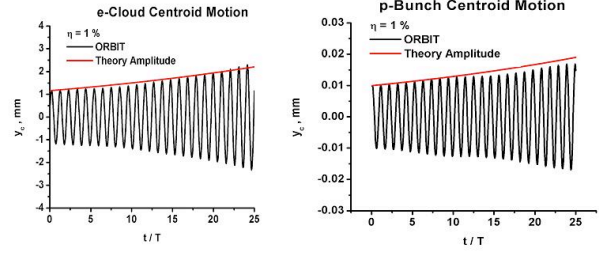


Fig. 8. Centroid oscillation of the two streams.

The horizontal axis, t/T , is the number of turns around the periodic structure. Both amplitudes grow at the same rate to maintain the same ratio, as expected ($|A_e/A_p|$ for $\eta = 0.01$). To simulate 10 turns in this periodic structure requires about 10 minutes using the 16 CPUs of the SNS cluster.

The growth rate, calculated from the first harmonic of the proton bunch centroid, increases with increasing neutralization factor (Fig. 9). For large neutralization factors, we can apply the analytic two stream model only for the first several turns because the electron cloud quickly goes outside of the proton bunch stream.

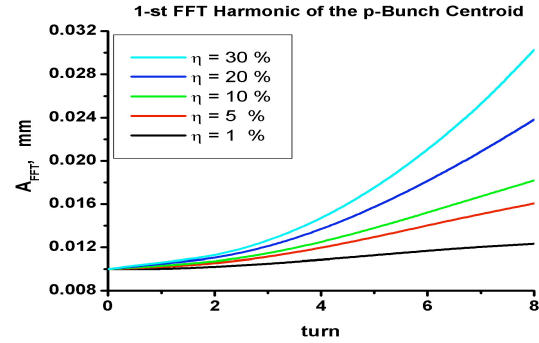


Fig. 9. The first harmonic of the proton bunch centroid versus turn number for different neutralization factors.

Results: Growth rate and neutralization factor

As seen in Fig. 10, the ORBIT growth rate is about 20% larger than the theory:

$$\frac{1}{\tau}_{theory} \approx \frac{Q_p \omega_0}{2} \sqrt{\frac{Q_e}{Q_p}} \propto \sqrt{\eta} \quad \text{for low } \eta \quad (8)$$

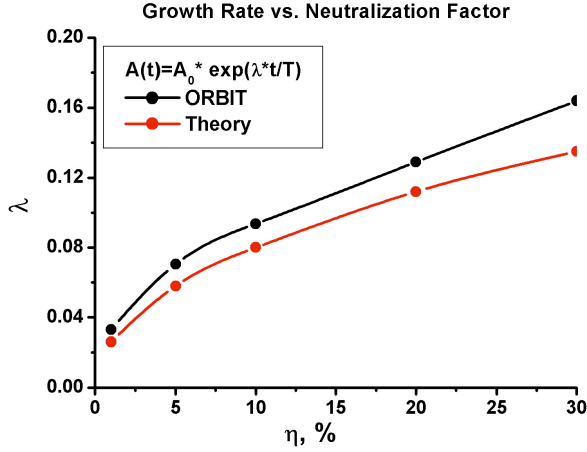


Fig. 10. Computational and theoretical growth rates versus neutralization factor.

These results are reasonably good, considering:

- The initial centroid modulation was determined from the two-stream model with $R_e = R_p = 30$ mm.
- We use $R_e = 26$ mm to ensure the linear force on the electrons.
- Each proton goes outside of the electron cloud during some part of its trajectory.
- The low neutralization factor case requires large amplitude ratio for the coherent oscillation, and it is hard to keep the electron cloud inside the proton bunch.

Using smaller computational grid-cell size could achieve more accuracy but this would require more macroparticles and calculation time. We consider this calculation to be sufficient as a benchmark test.

COMPUTATIONAL REQUIREMENTS FOR PSR BUNCHED BEAM CASE

For the two-stream model to PSR parameters (see Table I), the steams are the most unstable at $n_x = 83, n_y = 73$.

Taking the above into consideration, we estimate for the PSR bunched beam case:

- About 80×20 longitudinal nodes are needed to simulate the whole PSR ring.
- The simplest case with no boundary, no 3D proton-proton space charge, and no longitudinal momentum spread, will require about 80 times as much CPU time as our benchmark calculation.

This amounts to about 80 min. for 1 turn of PSR using the 16 CPU SNS cluster.

We need to activate the primary electron production and secondary emission surface instead of the linear neutralization factor.

Table 1: PSR parameters and two stream model

| | |
|-------------------------|---|
| Radii of electron cloud | $a_e = 12$ mm, $b_e = 15$ mm |
| Radii of proton beam | $a_p = 16$ mm, $b_p = 20$ mm |
| Energy of proton beam | 0.793 GeV |
| Proton line density | $\lambda_p = \frac{1.0 \times 10^{14}}{90.261 \text{ m}} = 1.108 \times 10^{12} [\text{m}^{-1}]$ |
| Betatron tune | $Q_x = 3.21, Q_y = 2.19$ |
| $Q_{e,x}$ | $Q_{e,x} = \frac{1}{\omega_0} \sqrt{\frac{4\lambda_p r_e c^2}{a_p(a_p + b_p)}} = 79.516$ |
| $Q_{e,y}$ | $Q_{e,y} = \frac{1}{\omega_0} \sqrt{\frac{4\lambda_p r_e c^2}{b_p(a_p + b_p)}} = 71.121$ |
| $Q_{p,x}$ | $Q_{p,x} = \frac{1}{\omega_0} \sqrt{\frac{4\lambda_e r_p c^2}{\gamma a_e(a_e + b_e)}} = 1.82\sqrt{\eta} \quad ; \eta = \frac{\lambda_e}{\lambda_p}$ |
| $Q_{p,y}$ | $Q_{p,y} = \frac{1}{\omega_0} \sqrt{\frac{4\lambda_e r_p c^2}{\gamma b_e(a_e + b_e)}} = 1.63\sqrt{\eta}$ |

CONCLUSION

The secondary emission surface model integrated into ORBIT, which is based on the model of Furman and Pivi, agrees with their spectrum results. A benchmark of the code with an analytic model for two-stream instabilities has been successfully done. We are going to simulate a PSR bunched beam case.

REFERENCES

- [1] A. Shishlo, Y. Sato, J. Holmes, S. Danilov and S. Henderson, "Electron-Cloud Module for the ORBIT code", Napa (CA, USA), April 2004, ECLLOUD'04, to be published.
- [2] M.A. Furman and M.T.F. Pivi, PRST-AB **5**, 124404 (2002).
- [3] M.T.F. Pivi and M.A. Furman, PRST-AB **6**, 034201 (2003).
- [4] R.J. Macek, A.A. Browman, M.J. Borden, D.H. Fitzgerald, R.C. McCrady, T. Spickermannn, and T.J. Zaugg, "Experimental Studies of Electron Cloud Effects at the Los Alamos PSR: a Status Report", Napa (CA, USA), April 2004, ECLLOUD'04, to be published.
- [5] D. Neuffer, E. Colton, D. Fitzgerald, T. Hardek, R. Hutson, R. Macek, M. Plum, H. Thiessen and T.S. Wang, NIM **A321**, 1-12 (1992).